Original Research Paper

Volume - 13 | Issue - 03 | March - 2023 | PRINT ISSN No. 2249 - 555X | DOI : 10.36106/ijar

Radiology

DIFFERENTIATION OF SOLID RENAL TUMOURS WITH MULTIPARAMETRIC MR IMAGING WITH HISTOLOGICAL CORRELATION

Dr. Parul Dutta	MD, DMRD, Professor Department of Radiology, Gauhati Medical College and Hospital, Guwahati- 781032
Dr. Parishmita Sarmah*	Junior Resident, Department of Radiology, Gauhati Medical College and Hospital. *Corresponding Author
Dr. Sasanka Kumar Barua	MS, MCh urology, Professor and Head, Department of Urology, Guwahati 781032.
Dr. Dipu Bhuyan	MD, Professor department of Radiology, Dhubri medical college and Hospital; Dhubri-783324
Dr. Sushant Agarwal	MD, DM, Associate professor Department of Radiology, Gauhati Medical college and hospital; Guwahati-781032

ABSTRACT **OBJECTIVES:** To identify the radiologic findings of the most common solid renal masses found in adult age group, illustrate imaging and histology correlates, and draw a clear diagnostic approach. **MATERIALS & METHODS:** 62 patients suspected to have solid renal masses were evaluated with mp-MRI. T2 SIR, ADC value and ADC ratio on DWI, SII on chemical shift imaging and wash in and wash out indices on dynamic contrast enhanced imaging were calculated for each tumor and the values were compared among different histologically proven renal tumors. **RESULTS:** ccRCC showed maximum T2 SIR whereas pRCC and lp-AML showed lowest mean T2 SIR. There is significant difference in SII of clear cell RCC (15.03±7.62) and non-clear cell renal cortical tumor (1.54±10.67), p<0.001. We found significant difference in mean tumor ADC of benign vs malignant lesions (p <0.006), higher stage (III & IV) vs lower stage (stage I &II) p <0.001. We found significant differences between clear cell and non-clear cell renal tumors in wash in indexes in all phases (p = 0.001) and late wash out index (p< 0.001). There is significant difference of papillary RCCs and other renal tumors in arterial and parenchymal WiI (p<0.001), early WoI (p=0.018) as well as late WoI (p<0.001). There is also significant difference between chromophobe RCCs and oncocytomas for arterial WiI (p=0.009), parenchymal and late WiI (p= 0.006); **CONCLUSION:** Multiparametric renal MRI is useful for differentiating solid renal tumors, predict their histologic grading and thus guide further management.

KEYWORDS : Solid renal tumor, multiparametric MRI, diffusion weighted imaging, dynamic contrast enhanced imaging, histology.

INTRODUCTION:

In recent years because of increased use of high-resolution cross-sectional imaging, there has been an increase in incidental solid renal masses. This necessitates additional imaging characterization for accurate diagnosis and proper management.

Renal cell carcinoma (RCC) is responsible for 3% of all adult cancers and 85% of all kidney tumors (1). Incidence of RCC is lower in Asian region compared to the western countries, particularly in India, possibly due to lack of organized data and reporting system. RCC can be categorized into clear cell renal carcinoma (ccRCC), papillary renal carcinoma(pRCC), chromophobe carcinoma (chRCC), collecting duct renal carcinoma, medullary and unclassified renal carcinoma, according to the First International Workshop on RCC sponsored by the World Health Organization. Because of the overlapping imaging characteristics and heterogeneity of imaging features as well as, the lack of reliable imaging criteria for recognition of various renal tumors, accurate diagnosis remains a challenge. Two main benign lesions may be challenging to distinguish from RCC, these are oncocytomas, which account for 3–7% of all renal tumors, and angiomyolipoma (AML), specifically the lipid-poor subtype, which are generally the most prevalent benign solid renal neoplasms (2,3).

MRI is frequently utilized to characterize renal tumors that are unclear on US and CT. Renal multiparametric MR imaging allows estimation of fat content of lesion, intra-lesion vascularity and diffusion restriction and may allow differentiation of malignant from benign lesions, classify RCC subtypes and predict histologic grades (4).

The purpose of this study is to review the characteristic MR imaging features of solid renal masses including RCC and common benign renal masses, correlating it with histology of extirpated tumors and propose a diagnostic imaging approach for evaluation of solid renal masses using multiparametric MR imaging.

AIMS AND OBJECTIVES:

1. To draw a clear diagnostic approach for solid renal masses using multiparametric MR imaging.
2. Identify and describe the spectrum of radiologic findings of the most common solid renal masses found in adult age group.
3. Illustrate imaging and histology correlates of the most common solid renal masses.

Subjects and Methods:

Patients:

It was a hospital-based prospective observational study done in department of Radiodiagnosis, Gauhati Medical College and Hospital, from April 2021 to June 2022 after approval of the institutional Ethical Committee. All adult patients who are suspected to have solid renal mass after clinical examination or initial evaluation with USG and CT were included in the study. Patients already on treatment for RCC or patients having cystic renal masses were excluded from the study. All the patients had initially undergone CECT thorax and abdomen for exclusion of macroscopic fat containing lesions like angiomyolipoma, cystic renal masses, infective etiology including abscess and detection of metastasis. Initially, a total of 65 patients were selected in the study, out of which two patients were excluded as contrast could not be administered due to high Sr. creatinine and one was excluded from the study because of inconclusive HPE report.

Data collection:

Study data consisted of demographic features of patients, ADC value and SI measurements, SI ratio of renal masses and renal parenchyma in CE-MRI phases, and the surgical and pathological findings of renal masses. A total of 62 renal masses included in the study. The patients underwent multiparametric MRI which was performed within 1 week of expected day of surgery or prior to commencement of treatment. Type of solid renal tumor was subsequently confirmed on histopathological examination of surgical specimens of 55 patients and biopsy specimen of 7 patients.

Imaging protocol:

Magnetic resonance imaging (MRI) evaluation was performed on MAGNETOM SKYRA 3 Tesla MRI machine and analysis and processing was done in SYNGO SOFTWARE by Siemans. All patients were subjected to 8 hours of fasting prior to the scan. Patients were scanned in the supine position by using a body matrix coil. T2W (HASTE) transverse, coronal, and sagittal images, T2W blade-fat-saturated transverse, T1W in and opposed phase transverse and DW transverse images at three b gradients (b 50, 500 and 800 s/mm2) were obtained before administration of contrast agent. A transverse three-dimensional fat-saturated T1W interpolated spoiled gradient-echo sequence (VIBE: volumetric interpolated breath-hold examination) was obtained dynamically in the corticomedullary, nephrographic phases after administration of a bolus of 0.1 mmol/kg of body weight gadobutrol (Gadovist) at a rate of 2 mL/s followed by a 20 mL saline flush. Images were obtained in arterial phase, parenchymal phase and delayed phase after 35-40 seconds, 60–80 seconds and 3-5 mins of intravenous (IV) contrast agent administration respectively. Pre-contrast and postcontrast T1W images were obtained as breath-hold sequences. Finally, late-phase coronal and transverse fat-saturated spin-echo T1W images were obtained and examinations. Imaging parameters are presented in Table 1.

Table 1: MP-MRI imaging parameters

MR Sequence		TR/TE (ms)	Flip Angle (°)	FOV (mm)	Matrix
T2-weighted HASTE	Coronal	1400/100	151	280	256x256
	Sagittal	1400/100	152	310	
	Axial	1400/96	160	300	320x203
T1-VIBE-fat-saturated coronal		3.8/1.3	70	380	384x270
T1-VIBE-DIXON axial	Opposed phase imaging	4/1.3	9	380	320x240
	In-phase imaging	4/2.5	9	380	320x240
Diffusion-weighted Imaging axial	b-value=50, 500 and 800	5300/51	--	380	192x116
T1-weighted fat-suppressed gradient-echo (VIBE), before and after contrast administration		4/1.3	9	380	320x195

Image analysis:

MRI data for each of the 62 renal masses were assessed and imaging diagnosis was given prior to the review of pathological findings. The maximum tumor diameter was measured at the site of the maximum tumor area on T2-weighted (T2W) axial images. For the quantitative analysis, we used the method described by Cornelis et al. (5). For this purpose, an identical ROI was drawn on tissue components of each tumor, which were assessed on contrast-enhanced T1- and T2-weighted images.

The signal intensity ratio was calculated using the following equation:

SIR = (SItum / SIkid) × 100; where SIR is the signal intensity ratio, SItum is the signal intensity of the tumor and SIkid is the signal intensity of the ipsilateral kidney.

On chemical shift imaging the change of SI was quantified using the T1 SI index (SII),

SII=[(TuSIin −TuSIopp)/(TuSIin)]×100; where TuSIin is tumor SI on in-phase images and TuSIopp is tumor SI on opposed-phase images.

DW images at b values of 50, 500, and 800 s/mm2 were obtained in the axial plane before IV contrast agent administration. The region of interest (ROI) was localized in renal masses and normal-appearing renal parenchyma on ADC maps. In cases of renal lesions not showing diffusion restriction, the ROI was placed in the most homogeneous portion avoiding the possible area of necrosis. The ADC value from single ROI was considered as the representative ADC of the renal lesion. The ADC ratio was calculated for each tumor defined as follow: ADCr = (ADC tumour/mean ADC of ipsilateral kidney)×100.

On DCE-MRI, signal intensity measurements were performed in renal masses on pre-contrast and postcontrast images at arterial, parenchymal and delayed phases. The ROI was placed within the most enhancing portion of the tumor based on a visual assessment in solid masses. Measurements were performed from the same localization on all sequences of pre-contrast and post contrast MR images. Three contrast-enhanced wash-in indexes were calculated depending on the contrast-enhanced phase using equation:

Wash-in index = (SIenh - SIunenh) / SIunenh × 100; SIenh is the signal intensity on contrast enhanced images and SIunenh is the signal intensity on unenhanced images. An early arterial wash-in index using the contrast-enhanced arterial phase, a parenchymal wash-in index using the parenchymal phase, and a late wash-in index using the excretory phase were obtained.

Initial washout index for the parenchymal phase was calculated as follows:

Washout index = (SIparen -SIart) / SIart × 100,

Where, SIparen is the signal intensity in the parenchymal phase and SIart is the signal intensity in the arterial phase. A second, later washout index was obtained between the arterial and excretory phases by substituting the variable SIlate (signal intensity in the excretory phase) for SIart in equation.

Also, other tumor characteristics on imaging like site, location, size, margin of tumor, whether tumors were exophytic or endophytic, presence of capsular invasion, necrosis and renal vein or IVC invasion were analyzed.

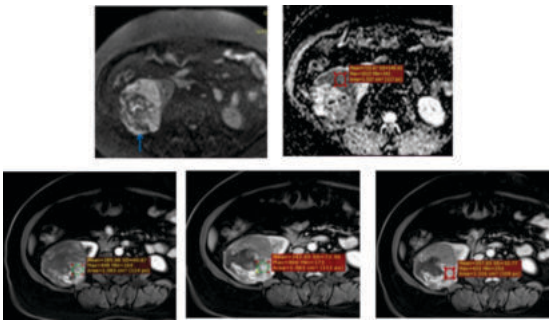

Figure 1: Case of papillary RCC, Top row: DWI showing selection of ROI in ADC measurement. Bottom row from left showing selection of ROI and measurement of signal intensity in arterial, parenchymal and delayed phases respectively.

Pathological analysis:

Histopathological diagnosis was available for all tumors after either a surgical excision (n=55) or percutaneous biopsy using an 18-gauge automated side-cutting needle (n=7). No unclassified RCCs were reported. The pathologists were blinded to the MRI findings and analyzed the histopathology of renal tumor, Fuhrman nuclear grade, lymphovascular invasion, perilesional invasion and lymph node positivity.

Statistical analysis:

Statistical analysis was done. All data were analyzed using IBM SPSS V21, Graph Pad Prism and Microsoft excel. Chi square test is used to evaluate association between categorical variables. Diagnostic accuracy test and ROC Curve is used to evaluate sensitivity and specificity, PPV, NPV and accuracy. Data were checked for normality using Kolmogorov-Smirnova and Shapiro-Wilk test. Independent T test is used to compare mean difference between two group and ANOVA is used for more than two groups depending on fulfilment of normality assumption for continuous variables. A p value <0.05 was considered as statistically significant at 95% confidence interval.

RESULTS:

Out of the 62 study subjects, 44 were male (71%) and 18 were female (29%). The mean and standard deviation was 55.1+10.6 years, most of the patients were in the 50-59 age group (n: 22, 35.5%) followed by 60-

69 age group (n: 15, 24.1%). Sixty-two renal masses (malignant: 57, benign: 5) were evaluated which included ccRCC (n: 38), pRCC (n: 9), chRCC (n: 5), LP-AMLs (n: 2), oncocytomas (n: 3), spindle cell carcinoma (n: 1), lymphoma (n:3) and metastatic adenocarcinoma (n: 3). The mean tumor size of benign lesions was 4.4 ±1.3 (maximum: 6 cm, minimum: 2.8 cm); whereas the mean tumor size of malignant tumors is 6.6±3.5 (maximum 15 cm, minimum: 1.4 cm), p (0.18).

On T2 weighted imaging, most of the clear cell RCC showed hyperintense signal intensity with maximum mean SIR of 139.2 (maximum: 173.66, minimum: 103.02), papillary RCC and lipid poor-AML mostly showed hypointense signal intensity with mean SIR of 44.87 and 55.1 respectively. ChRCC and oncocytoma also showed moderate T2 hyperintensity with mean SIR of 130.68 and 107.61 respectively. On chemical shift imaging, maximum SII was observed with lipid poor AML with SII of 33.85, clear cell RCC also showed signal drop on opposed phase with mean SII of 15.03±7.6. Mean SII of all non-clear renal tumor was found to be 1.54±10.67. T2 SIR, mean tumor ADC and SII of different renal tumors are shown in table 2.

Table 2: Mean T2 SIR, mean tumor ADC and mean SII of different renal tumors

	ccRcc	pRcc	chRcc	Oncocytoma	Lp-AML	others	p value
Mean T2 SIR	139.20	44.87	130.68	107.61	55.18	76.77	<0.001
Mean Tumour SII	15.03	-5.18	1.71	-1.26	33.85	1.00	<0.001
Mean tumor ADC	1.40	0.86	1.22	2.066	1.3	0.95	<0.001

ROC curve based on tumor T2 SIR and SII is shown in figure 2. The optimal cut-off value based on T2 SIR is 106.08 with AUC 0.915, sensitivity 92.1% and specificity of 79.2% for differentiating clear cell RCC from non-clear cell tumors. The best cut-off value based on tumor SII value is 4.4 with sensitivity of 92.1% and specificity of 91.7% for diagnosing clear cell RCC from non-clear cell tumors.

On diffusion weighted MRI, the mean tumor ADC of malignant masses were found to be 1.27±0.37 and mean tumor ADC of benign tumor was 1.76±0.44 (p=0.006); mean renal parenchymal ADC in case of malignant lesion was found to be 1.73± 0.11 and that of benign lesion was 1.94±0.21 with ADC ratio of 86.53±12.29 for malignant lesion and 71.21±16.78 for benign lesion (p=0.051). Among malignant lesions papillary variant showed lowest mean tumor ADC value of 0.86, followed by others including spindle cell carcinoma, lymphoma and metastatic carcinoma (0.95), chromophobe RCC (1.22) and clear cell RCC (1.40), p<0.01. Least diffusion restriction was observed with oncocytoma with mean tumor ADC value of 2.06. The size and grade of RCC correlated inversely with ADC value. Larger and high-grade tumor showed low mean tumor ADC value compared to smaller and low-grade tumors. Histologically proven high grade tumor showed mean ADC of 1.1 whereas low grade RCC showed mean ADC of 1.4. The ROC curve based on ADC and ADC ratio for tumor grade is shown in figure 3. The optimal cut-off value based on tumor ADC is 1.35 with AUC 0.753, sensitivity 85.7% and specificity of 64.5% for differentiating high grade and low-grade tumors. Figure 4, bar diagram with SD shows correlation of stage of RCC with mean tumor ADC. Stage I+II showed mean tumor ADC of 1.44 whereas stage III+IV showed mean tumor ADC of 1.03, p<0.001.

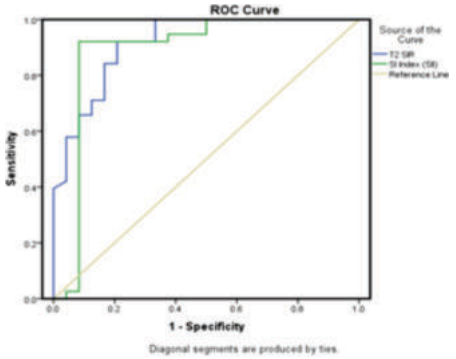

Figure 2: ROC curve based on tumor T2 SIR and SII

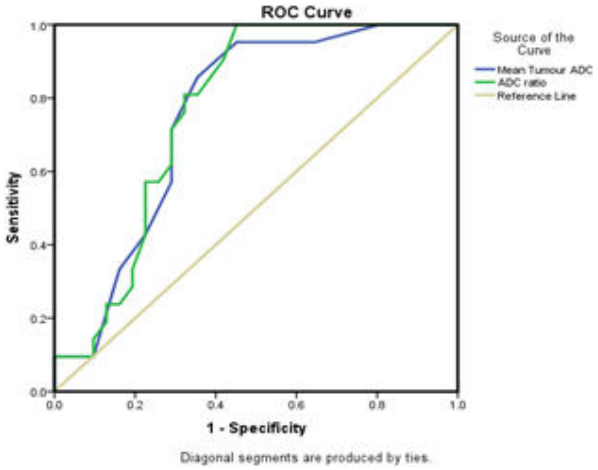

FIGURE 3: ROC curve based on ADC and ADC ratio for tumor grade

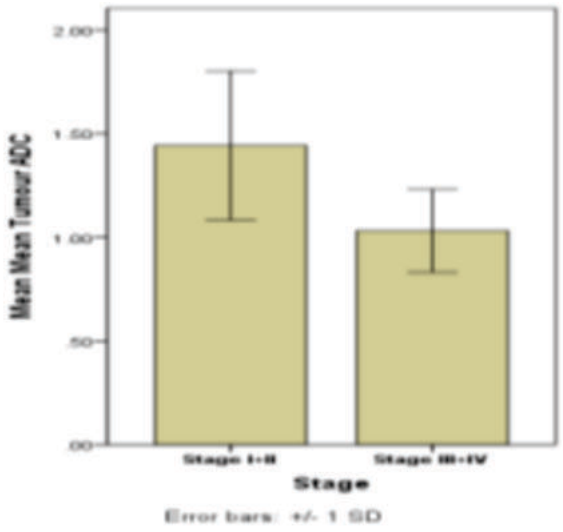

FIGURE 4: Bar diagram with SD showing stage of RCC with mean tumor ADC

On dynamic contrast enhanced MRI, the mean arterial, parenchymal and late wash in indices and early and late wash out indices of different tumors are shown in Table 3. We found significant difference in arterial (p=0.01), parenchymal (p=0.03) and delayed WiI (p=0.01) of benign and malignant tumors; however, no significant difference was observed in WoI of benign and malignant tumors (p=0.62 and p=0.89 in early and late WoI respectively). We found that SI values measured on arterial phase were more useful in differentiating among renal lesions.

Among RCC subtypes, papillary RCCs showed the lowest mean arterial (41.1) and parenchymal (61.37) WiI. We found significant differences between clear cell and non-clear cell renal tumors in WiI in all phases (p = 0.001) and late WoI (p< 0.001). In parenchymal phase, the AUC, sensitivity and specificity are .820, 84.2% and 70.8% respectively, for differentiation of clear cell RCC from non-clear cell RCC.

No significant difference was found in arterial WiI and parenchymal WiI of clear cell RCC and oncocytoma, p=0.44 and p=0.66 respectively. However, significant difference was seen in late WiI (p=0.025), early WoI(p=0.024) and late WoI (p=0.005) for differentiating clear cell from oncocytoma. There is significant difference of papillary RCCs and other renal tumors in arterial and parenchymal WiI (p<0.001), early WoI (p=0.018) as well as late WoI (p<0.001). There is also significant difference between chromophobe RCCs and oncocytomas for arterial WiI (p=0.009), parenchymal and late WiI (p= 0.006); however, no significant difference was found in wash out indices. We also found significant difference between clear cell RCCs and oncocytomas for late WiI (p = 0.025), early WoI (p=0.024) as well as late WoI (p=0.005).

Table 3: Mean wash in index and wash out index of different tumors in study group

	ccRCC	pRCC	chRCC	Oncocytoma	Lp-AML	others
Mean Arterial WiI	126.82± 25.22	41.19± 15.96	80.95 ±24.97	138.28 ±5.56	166.31 ±24.07	42.71 ±5.22
Mean Parenchymal WiI	136.89± 28.3	61.37 ±21	70.7 ±38.97	168.2 ±8.77	142.05 ±29.3	67.92 ±7.9
Mean Late WiI	100.26± 28.6	71.15 ±20.6	47.51 ±36.34	139.3 ±6.7	111.57 ±51.2	38±8.22
Mean Early WoI	4.49± 5.83	14.25 ±7.51	-5.87 ±17.03	12.57 ±3.6	-9.23 ±2.8	17.13 ±7.22
Mean Late WoI	-11.84 ±7.08	21.26 ±6.76	-18.56 ±17.56	0.514 ±5.1	-21.1 ±12.1	-5.99 ±9.22

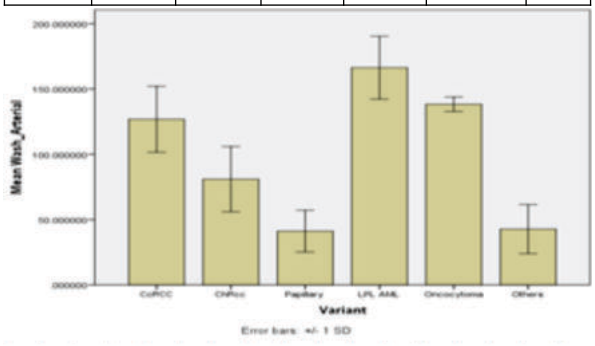

FIGURE 5: Bar diagram with SD showing arterial wash in index of different renal tumors

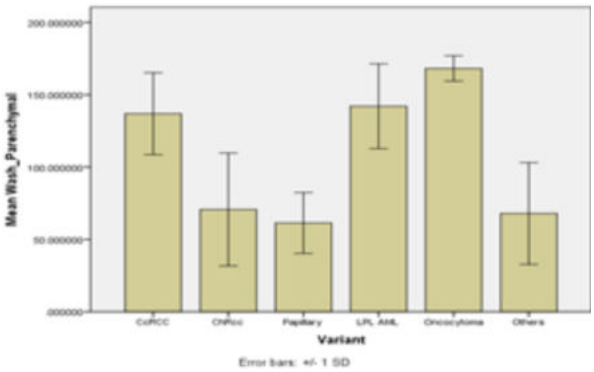

FIGURE 6: Bar diagram with SD showing parenchymal wash in index of different renal tumors

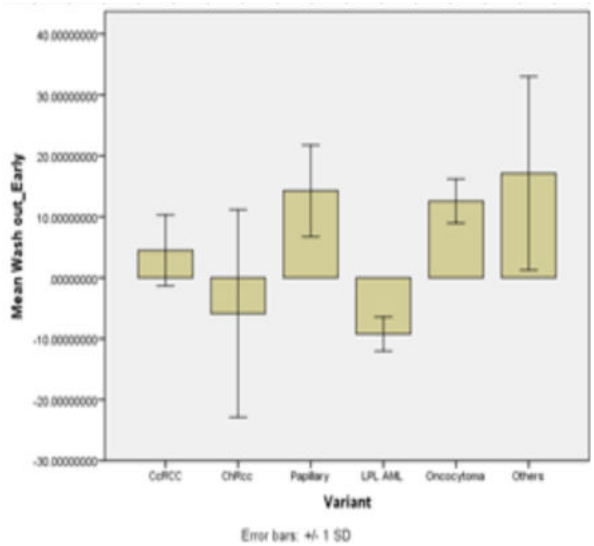

FIGURE 7: Bar diagram with SD showing early wash out index of different renal tumors

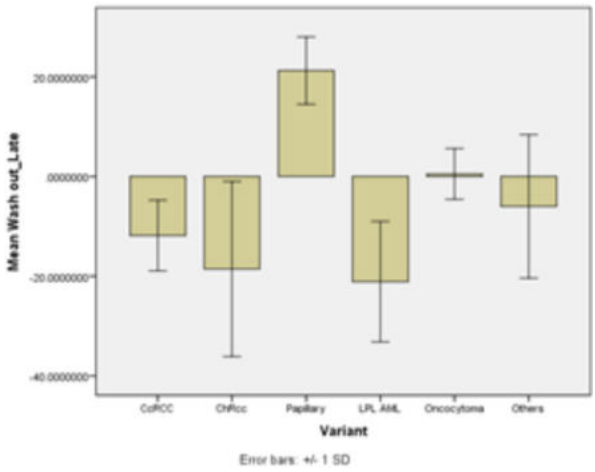

FIGURE 8: Bar diagram with SD showing late wash out index of different renal tumors

DISCUSSION:

In our study, we found that on T2-WI, most of the clear cell RCC were hyperintense; most papillary RCCs were hypointense with mean T2 SIR of 44.87±10.46 which was significantly different from all other renal cortical tumors combined (mean T2 SIR of 126.61±30.66; p <0.001), which corroborates with the findings of Oliva et al.(6).

In our study, we found that there is significant difference in SII of clear cell RCC (15.03±7.62) and non-clear cell renal cortical tumor (1.54±10.67), p<0.001, this corroborates with the finding of Yoshimitsu et al. and Jhaveri et al.(7,8). At a cut-off value of 4.44, there was sensitivity of 92.1% and specificity of 91.7% in diagnosing clear cell RCC.

ADC values detected in our study were more restricted, ranging from 0.6 to 2.2x10-3mm2/s because of exclusion of cystic and infectious lesions. Our study had relative low number of benign tumors comprising of only oncocytoma and lipid poor AML. Lipid rich AML does not provide a diagnostic challenge because of easy detection of macroscopic fat on non-contrast as well as contrast enhanced CT and signal drop on fat saturated MR images. We found significant difference between mean tumor ADC of benign lesions (1.76±0.44 x 103 mm2/sec) and malignant lesions (1.27±0.37 x 103 mm2/sec) (p <0.006) which correlates with that conducted by Taouli et al. (9). We also found that there is significant difference between mean ADC of clear cell RCC (1.41±0.34 x 10-3 mm2/sec) and other renal tumors (1.15±0.42 x 10-3 mm2/sec), p =0.009 that correlates with study conducted by Hoetker et al.(10) and Elsorougy et al.(11).

Sandrasegaran et al.(12) showed that the ADCs of high-grade clear cell cancers (Fuhrman grades III and IV) tended to be lower than those of low-grade clear cell cancers. We found that ADCs of high grade RCC (Fuhrman grades III and IV) are lower than that of low grade RCCs (1.1 vs 1.4 × 10–3 mm2/s), p=0.005.

We also assessed the contrast enhancement parameters of renal masses on different phases of CE-MRI with signal intensity measurements. We found significant differences between clear cell and non-clear cell renal tumors in wash in indexes in all phases (p = 0.001) and late wash out index (p< 0.001). In parenchymal phase, the AUC, sensitivity and specificity are .820, 84.2% and 70.8% respectively, for differentiation of clear cell RCC from non-clear cell RCC. There is significant difference of papillary RCCs and other renal tumors in arterial and parenchymal WiI, early WoI as well as late WoI. We also found significant difference between clear cell RCCs and oncocytomas for late WiI (p = 0.025), early WoI (p=0.024) as well as late WoI (p=0.005). Our study correlates with that conducted by Cornelis et al. (5) who found significant differences between papillary RCCs and other renal tumors for arterial WiI, initial WoI. They also found significant difference between chromophobe RCCs and oncocytomas for parenchymal and late WiI, as well as early and late WoI. Galmiche et al. showed that wash-in indexes in the arterial and parenchymal phases were significantly different between the chromophobe RCC and oncocytoma (13). We found significant difference between chromophobe RCCs and oncocytomas for arterial WiI, parenchymal and late WiI.

Our study had some limitations, firstly, the number of benign lesions were significantly less due to exclusion of abscesses, pyelonephritis and classic AML by prior CECT. Secondly, the small number for some tumor variants could also limit the conclusion of this study. Third, although MR characterization is more frequently utilized for small renal masses (3-4 cm), our study also included large lesions.

CONCLUSION:

In conclusion, we have identified certain MR features that correlate with findings at histology and pathology. Our study demonstrated that using a quantitative multiparametric MRI approach, in contrast to using any single MRI parameter, that combines T2WI, DWI, chemical shift and contrast-enhanced imaging improves the discrimination of various renal tumors including clear cell RCC from that of less aggressive tumors subtypes and may be crucial in risk stratification and treatment choice in the care of patients with renal cortical tumors.

CONFLICT OF INTEREST: No conflict of interest to declare.

FINANCIAL DISCLOSURE: The study has received no financial support.

ABBREVIATIONS:

RCC – Renal Cell Carcinoma
ccRCC - Clear Cell Renal Cell Carcinoma
chRCC – Chromophobe Renal Cell Carcinoma
pRCC- Papillary Renal cell Carcinoma
lp-AML: Lipid poor angiomyolipoma
DWI: Diffusion weighted imaging
DCE: Dynamic contrast enhanced
WiI: Wash in index
WoI: Wash out index

REFERENCES:

1. Ljungberg B, Campbell SC, Choi HY, Cho HY, Jacqmin D, Lee JE, et al. The epidemiology of renal cell carcinoma. Eur Urol. 2011 Oct;60(4):615–21.
2. Perez-Ordonez B, Hamed G, Campbell S, Erlandson RA, Russo P, Gaudin PB, et al. Renal oncocytoma: a clinicopathologic study of 70 cases. Am J Surg Pathol. 1997 Aug;21(8):871–83.
3. Amin MB, Crotty TB, Tickoo SK, Farrow GM. Renal oncocytoma: a reappraisal of morphologic features with clinicopathologic findings in 80 cases. Am J Surg Pathol. 1997 Jan;21(1):1–12.
4. Ramamurthy NK, Moosavi B, McInnes MDF, Flood TA, Schieda N. Multiparametric MRI of solid renal masses: pearls and pitfalls. Clin Radiol. 2015 Mar;70(3):304–16.
5. Cornelis F, Tricaud E, Lasserre AS, Petitpierre F, Bernhard JC, Le Bras Y, et al. Routinely performed multiparametric magnetic resonance imaging helps to differentiate common subtypes of renal tumours. Eur Radiol. 2014 May;24(5):1068–80.
6. Oliva MR, Glickman JN, Zou KH, Teo SY, Mortelé KJ, Rocha MS, et al. Renal cell carcinoma: t1 and t2 signal intensity characteristics of papillary and clear cell types correlated with pathology. AJR Am J Roentgenol. 2009 Jun;192(6):1524–30.
7. Yoshimitsu K, Honda H, Kuroiwa T, Irie H, Tajima T, Jimi M, et al. MR detection of cytoplasmic fat in clear cell renal cell carcinoma utilizing chemical shift gradient-echo imaging. J Magn Reson Imaging JMRI. 1999 Apr;9(4):579–85.
8. Jhaveri KS, Elmi A, Hosseini-Nik H, Hedgire S, Evans A, Jewett M, et al. Predictive Value of Chemical-Shift MRI in Distinguishing Clear Cell Renal Cell Carcinoma From Non–Clear Cell Renal Cell Carcinoma and Minimal-Fat Angiomyolipoma. Am J Roentgenol. 2015 Jul 1;205(1):W79–86.
9. Taouli B, Thakur RK, Mannelli L, Babb JS, Kim S, Hecht EM, et al. Renal lesions: characterization with diffusion-weighted imaging versus contrast-enhanced MR imaging. Radiology. 2009 May;251(2):398–407.
10. Hötker AM, Mazaheri Y, Wibmer A, Karlo CA, Zheng J, Moskowitz CS, et al. Differentiation of Clear Cell Renal Cell Carcinoma From Other Renal Cortical Tumors by Use of a Quantitative Multiparametric MRI Approach. AJR Am J Roentgenol. 2017 Mar;208(3):W85–91.
11. Elsorougy A, Farg H, Bayoumi D, El-Ghar MA, Shady M. Quantitative 3-tesla multiparametric MRI in differentiation between renal cell carcinoma subtypes. Egypt J Radiol Nucl Med. 2021 Feb 5;52(1):49.
12. Sandrasegaran K, Sundaram CP, Ramaswamy R, Akisik FM, Rydberg MP, Lin C, et al. Usefulness of diffusion-weighted imaging in the evaluation of renal masses. AJR Am J Roentgenol. 2010 Feb;194(2):438–45.
13. Galmiche C, Bernhard JC, Yacoub M, Ravaud A, Grenier N, Cornelis F. Is Multiparametric MRI Useful for Differentiating Oncocytomas From Chromophobe Renal Cell Carcinomas? AJR Am J Roentgenol. 2017 Feb;208(2):343–50.